THE TANGENT STIFFNESS MATRIX OF A CONSTANT VELOCITY JOINT

Bruce Minaker
Department of Mechanical, Automotive, and Materials Engineering, University of Windsor, Windsor, ON, Canada
Email: bminaker@uwindsor.ca

ABSTRACT

In the ongoing search for mathematically efficient methods of predicting the motion of vehicle and other multibody systems, and presenting the associated results, one of the avenues of continued interest is the linearization of the equations of motion. While linearization can potentially result in reduced fidelity in the model, the benefits in computational speed often make it the pragmatic choice. This paper discusses the tangent stiffness matrix, those terms in the stiffness matrix that result from preloads in a multibody system, at the point of linearization. In this case, the focus is on the tangent stiffness matrix of constant velocity joints. The general form of the matrix is presented, and verified through comparison with several other dynamically equivalent systems.

Keywords: constant velocity; tangent stiffness; equations of motion; multibody dynamics; linearization.

RÉSUMÉ

Dans la recherche continue de méthodes mathématiquement efficaces pour prédire le mouvement d'un véhicule et d'autres systèmes multi-corps, et pour présenter les résultats associés, l'une des voies d'intérêt continu est la linéarisation des équations du mouvement. Alors que la linéarisation peut potentiellement entraîner une fidélité réduite dans le modèle, les avantages de la vitesse de calcul en font souvent un choix pragmatique. Cet article traite de la matrice de rigidité tangente, ces termes de la matrice de rigidité qui résultent des précharges dans un système à corps multiples, au point de linéarisation. Dans ce cas, l'accent est mis sur la matrice de rigidité tangente des joints homocinétiques. La forme générale de la matrice est présentée et vérifiée par comparaison avec plusieurs autres systèmes dynamiquement équivalents.

Mots-clés : vitesse constante ; rigidité tangente ; équations de mouvement ; dynamique multi-corps ; linéarisation.

1. INTRODUCTION

In the ongoing search for mathematically efficient methods of predicting the motion of vehicle and other multibody systems, and presenting the associated results, one of the avenues of continued interest is the linearization of the equations of motion. While linearization can potentially result in reduced fidelity in the model, the benefits in computational speed often make it the pragmatic choice. Furthermore, linearizaton opens additional avenues of analysis, such as eigenvalue/eigenvector decomposition, frequency response, and linear quadratic control (LQR/LQG).

This work relates to the ongoing development of a multibody dynamics based vehicle motion simulation, based on the equations of motion generator code EoM, developed by the University of Windsor Vehicle Dynamics and Control research group [1][2], although the results would be equally applicable in any similar implementation. The EoM software is able to generate equations of motion for complex three dimensional multibody systems, but restricts the result to linear equations.

When generating the linearized equations of motion as ordinary differential equation (ODEs), many authors will choose to present them in the traditional linear second order form shown in Eq. (1).

$$\mathbf{M}\ddot{\boldsymbol{q}} + \mathbf{L}\dot{\boldsymbol{q}} + \mathbf{K}\boldsymbol{q} = \boldsymbol{Q}_{\mathrm{e}} \tag{1}$$

In this form, the matrices **M**, **L**, and **K** represent the mass, damping, and stiffness respectively, $\boldsymbol{q}$ is the vector of generalized coordinates, and $\boldsymbol{Q}_{\mathrm{e}}$ is the vector of external generalized forces. In this traditional form, it is assumed that the equations are presented in minimal coordinates, that is, the number of degrees of freedom equals the number of second order equations and the number of coordinates.

In order to understand how the stiffness matrix is computed in the EoM software, it is important to note the way in which it prepares the equations of motion. The formulation implemented by EoM uses redundant coordinates and constraints, as shown in Eq. (2),

$$\mathbf{M}_{\mathrm{r}}\ddot{\boldsymbol{x}} = \boldsymbol{f} + \boldsymbol{f}_{\mathrm{c}} \tag{2}$$

where $\boldsymbol{x}$ is the vector of all possible translational and rotational motions, $\boldsymbol{f}$ is the vector of forces and moments, including external applied forces, inertial or gyroscopic forces, or those due to the deflection of flexible connecting elements. The vector of constraint forces and moments $\boldsymbol{f}_{\mathrm{c}}$ that are imposed by the 'rigid' connectors, such as hinges or ball-joints, is treated as distinct. Note that the mass matrix in the two formulations is not the same; in the redundant coordinates approach, the matrix is larger by the amount of redundancy.

The equations of motion are supplemented by a set of constraint equations that are formed to enforce the various connections. They are written as a vector function of the full set of coordinates, and equated to zero.

$$\boldsymbol{\phi}(\boldsymbol{x}) = \mathbf{0} \tag{3}$$

The constraint forces are expressed using the constraint Jacobian matrix and the Lagrange multipliers.

$$\boldsymbol{f}_{\mathrm{c}} = -\left[\frac{\partial \boldsymbol{\phi}}{\partial \boldsymbol{x}}\right]' \boldsymbol{\lambda} = -\boldsymbol{\phi}'_{\boldsymbol{x}}\boldsymbol{\lambda} \tag{4}$$

The stiffness matrix is found as a sum of the change in both the applied and constraint forces, as shown in Eq. (5).

$$\mathbf{K} = -\left[\frac{\partial \boldsymbol{f}_{\mathrm{c}}}{\partial \boldsymbol{x}} - \frac{\partial \boldsymbol{f}}{\partial \boldsymbol{x}}\right] = \left[\frac{\partial(\boldsymbol{\phi}_{\boldsymbol{x}}'\boldsymbol{\lambda})}{\partial \boldsymbol{x}} - \frac{\partial \boldsymbol{f}}{\partial \boldsymbol{x}}\right] \tag{5}$$

When computing the derivatives in Eq. (5), the Lagrange multipliers are treated as constant values. Any effect of changing Lagrange multipliers is eliminated along with the redundancy in the equations when they are reduced to minimal coordinates. In the general case, the constraint forces at equilibrium can vary depending on the specifics of the system, and are computed in advance for later use in the generation of the equations of motion. It is also noteworthy that in EoM, the equations are written in the local frame of each body, so weight forces will change direction as the body rotates. In this fashion, the effect of the constraint forces will be captured in the first term, and the effect of the weight force will be captured in the second, but both are needed to form the complete stiffness matrix.

1.1. Tangent stiffness

The first term is in the stiffness matrix is known as a *tangent stiffness* matrix. The tangent stiffness matrix is due to changes in direction of the constraint forces, and not their magnitude. The vector $\boldsymbol{\lambda}$ is evaluated at equilibrium, so the tangent stiffness matrix requires that the preloads be determined prior to generation of the equations of motion, e.g., using static equilibrium. If there is no preload in the mechanism at equilibrium, the tangent stiffness term evaluates to zero. Consider, as an example, a massless link or wire that connects two rigid bodies, and maintains a fixed distance between its endpoints, as shown in Fig. 1. Application of Lagrange's equation, or one of many other equivalent approaches, will give a set of ordinary differential equations that can be linearized as shown in Eq. (6). The resulting stiffness matrix is shown in Eq. (7) and can be expanded as shown in Eqn. (8).

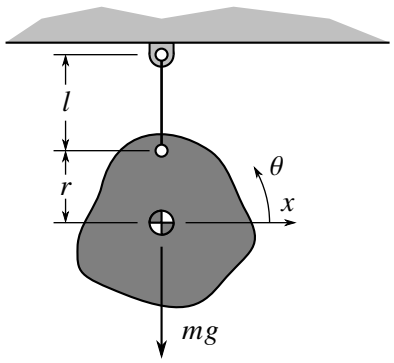

$$\begin{bmatrix} m & 0 \\ 0 & I_{\mathrm{G}} \end{bmatrix} \begin{Bmatrix} \ddot{x} \\ \ddot{\theta} \end{Bmatrix} + \frac{mg}{l} \begin{bmatrix} 1 & -r \\ -r & r^2 + rl \end{bmatrix} \begin{Bmatrix} x \\ \theta \end{Bmatrix} = \begin{Bmatrix} 0 \\ 0 \end{Bmatrix} \tag{6}$$

$$\mathbf{K} = \begin{bmatrix} mg/l & -mgr/l \\ -mgr/l & mg(r+l)r/l \end{bmatrix} \tag{7}$$

Fig. 1. An example system, a rigid body suspended by a massless link; in this case, the second body is the ground.

$$\mathbf{K} = \begin{bmatrix} 0 & -mg \\ 0 & mgr \end{bmatrix} + \begin{bmatrix} mg/l & -mgr/l \\ -mgr/l & mgr^2/l \end{bmatrix} + \begin{bmatrix} 0 & mg \\ 0 & 0 \end{bmatrix} = \begin{bmatrix} 0 & -mg \\ 0 & mgr \end{bmatrix} + \frac{mg}{l} \begin{bmatrix} 1 \\ -r \end{bmatrix} \begin{bmatrix} 1 \\ -r \end{bmatrix}' + \begin{bmatrix} 0 & mg \\ 0 & 0 \end{bmatrix} \tag{8}$$

The source of each of the terms in the expansion of the stiffness matrix is illustrated in Fig. 2.

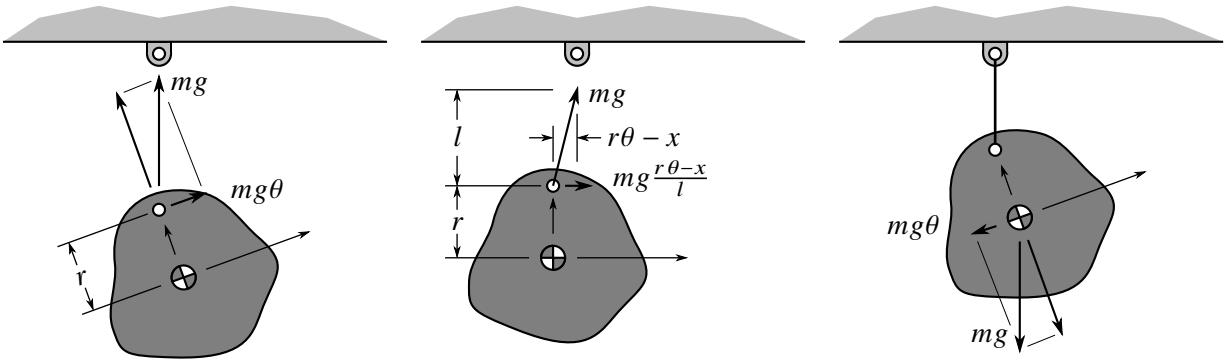

(a) first term in **K** (b) second term in **K** (c) third term in **K**

Fig. 2. Stiffness terms are generated due to: (a) the component of the constraint force (which in this case also equals mg) acting in the body fixed x axis, also generating a moment about the z axis, (b) the change in direction of the constraint force, generating both a force in the x axis and a moment about the z axis, and (c) the component of the weight force acting in the body fixed x axis.

The general tangent stiffness matrix for this wire or link type of constraint is 12×12, and can be computed using differentiation as shown in [2], giving the result shown in Eq. (9):

$$\mathbf{K} = -\begin{bmatrix} \mathbf{0} & \tilde{\boldsymbol{f}}_{\mathrm{g}} & \mathbf{0} & \mathbf{0} \\ \mathbf{0} & \tilde{\boldsymbol{r}}_1\tilde{\boldsymbol{f}}_{\mathrm{g}} & \mathbf{0} & \mathbf{0} \\ \mathbf{0} & \mathbf{0} & \mathbf{0} & -\tilde{\boldsymbol{f}}_{\mathrm{g}} \\ \mathbf{0} & \mathbf{0} & \mathbf{0} & -\tilde{\boldsymbol{r}}_2\tilde{\boldsymbol{f}}_{\mathrm{g}} \end{bmatrix} + \frac{f}{l}\begin{bmatrix} \tilde{\boldsymbol{u}} \\ \tilde{\boldsymbol{r}}_1\tilde{\boldsymbol{u}} \\ \tilde{\boldsymbol{u}}' \\ \tilde{\boldsymbol{r}}_2\tilde{\boldsymbol{u}}' \end{bmatrix}\begin{bmatrix} \tilde{\boldsymbol{u}} \\ \tilde{\boldsymbol{r}}_1\tilde{\boldsymbol{u}} \\ \tilde{\boldsymbol{u}}' \\ \tilde{\boldsymbol{r}}_2\tilde{\boldsymbol{u}}' \end{bmatrix}' \tag{9}$$

where $\hat{\boldsymbol{u}}$ is the unit vector along the link, $\boldsymbol{r}_1$ and $\boldsymbol{r}_2$ are the 'radius' vectors, i.e., the location of the endpoint of the link relative to the mass centre of each body, f is the tension force in the link, l is the length of the link, and $\boldsymbol{f}_{\mathrm{g}} = f\hat{\boldsymbol{u}}$. In all cases, the tilde notation is used to indicate the 3×3 skew symmetric matrix of the vector that is equivalent to a cross product, i.e., $\tilde{\boldsymbol{u}}\boldsymbol{a} = \hat{\boldsymbol{u}}\times\boldsymbol{a}$. A careful examination of the two terms shows that the first one is due to the change in direction of the link force relative to the body fixed frame as the body reorients, while the second is due to the change in direction of the tension force as the link reorients. A comparison shows that the first two terms in Eqn. (8) correspond to the two terms in Eq. (9), albeit considerably simplified due to the nature of the example problem (single body, planar motion). Not included in Eq. (9) is the effect of the weight force, which must be computed separately.

The tangent stiffness of a spherical joint is shown in Eq. (10). It is clearly identical to the first component of the result for the link in Eqn. (9), as the joint does not reorient, and only accounts for the change in direction of the body fixed reference frame.

$$\mathbf{K} = -\begin{bmatrix} \mathbf{0} & \tilde{\boldsymbol{f}}_{\mathrm{g}} & \mathbf{0} & \mathbf{0} \\ \mathbf{0} & \tilde{\boldsymbol{r}}_1\tilde{\boldsymbol{f}}_{\mathrm{g}} & \mathbf{0} & \mathbf{0} \\ \mathbf{0} & \mathbf{0} & \mathbf{0} & -\tilde{\boldsymbol{f}}_{\mathrm{g}} \\ \mathbf{0} & \mathbf{0} & \mathbf{0} & -\tilde{\boldsymbol{r}}_2\tilde{\boldsymbol{f}}_{\mathrm{g}} \end{bmatrix} \tag{10}$$

The tangent stiffness matrix of a hinge joint is again similar and shown in Eq. (11).

$$\mathbf{K} = -\begin{bmatrix} \mathbf{0} & \tilde{\boldsymbol{f}}_{\mathrm{g}} & \mathbf{0} & \mathbf{0} \\ \mathbf{0} & \tilde{\boldsymbol{r}}_1\tilde{\boldsymbol{f}}_{\mathrm{g}} - \tilde{\boldsymbol{u}}\tilde{\boldsymbol{u}}\tilde{\boldsymbol{m}}_{\mathrm{g}} & \mathbf{0} & \mathbf{0} \\ \mathbf{0} & \mathbf{0} & \mathbf{0} & -\tilde{\boldsymbol{f}}_{\mathrm{g}} \\ \mathbf{0} & \mathbf{0} & \mathbf{0} & -\tilde{\boldsymbol{r}}_2\tilde{\boldsymbol{f}}_{\mathrm{g}} + \tilde{\boldsymbol{u}}\tilde{\boldsymbol{u}}\tilde{\boldsymbol{m}}_{\mathrm{g}} \end{bmatrix} \tag{11}$$

The spherical and hinge joints are very similar, with the additional effects of the moment carried by the hinge joint ($\boldsymbol{m}_{\mathrm{g}}$), and the unit vector $\hat{\boldsymbol{u}}$ defines the axis of the rotation of the hinge, which is constant in both body fixed frames. Note that for a unit vector $\hat{\boldsymbol{u}}$, the identity in Eq. (12) holds.

$$\mathbf{I} + \tilde{\boldsymbol{u}}\tilde{\boldsymbol{u}} = \hat{\boldsymbol{u}}\hat{\boldsymbol{u}}' \Rightarrow -\tilde{\boldsymbol{u}}\tilde{\boldsymbol{u}} = \mathbf{I} - \hat{\boldsymbol{u}}\hat{\boldsymbol{u}}' \tag{12}$$

Note also that $\hat{\boldsymbol{u}}\hat{\boldsymbol{u}}'\boldsymbol{a}$ is the component of a vector $\boldsymbol{a}$ in the direction of $\hat{\boldsymbol{u}}$. This implies that $-\tilde{\boldsymbol{u}}\tilde{\boldsymbol{u}}\tilde{\boldsymbol{m}}_{\mathrm{g}}\boldsymbol{\theta}$ is the component of $\tilde{\boldsymbol{m}}_{\mathrm{g}}$ that results from the change in orientation, less any part of that change that lies along the axis of hinge. Of course, the hinge cannot carry any moment around its own axis (i.e., $\hat{\boldsymbol{u}}'\boldsymbol{m}_{\mathrm{g}} = 0$).

2. CONSTANT VELOCITY JOINTS

There term 'constant velocity' joint (CV joint) refers to one of several joints that are designed to transmit motion between rotating shafts that are misaligned. It is important to note the distinction between a CV joint and a universal joint (U-joint or Hooke joint). The universal joint has been commonly used in automotive applications for many years, notably in the drive shafts for rear wheel drive (RWD) vehicles. A single universal joint does not maintain a constant angular velocity relationship, but rather imposes a fluctuation in output speed. The magnitude of the fluctuation is a function of the angle of misalignment. By combining pairs of universal joints, the fluctuation can be cancelled, to achieve a constant velocity relationship, but requires that the two universal joints are phased properly on the shaft.

As the automotive industry made the transition from RWD to front wheel drive (FWD), CV joints became more popular for use in front axles. Most FWD vehicles today use a pair of CV joints on each axle, but typically they are of different types. The inboard joint, closest to the transmission, is commonly called a 'tripot' joint, while the outer joint, at the wheel, is typically a 'Rzeppa' [3] style joint. The joints differ in their construction, with the Rzeppa joint being significantly more complex to produce, as it requires complex spatial surfaces to be machined during manufacture. In fact, the tripot joint is not truly a CV joint, see Urbinati and Pennestrì [4], and is restricted to use on the inboard end due to the much lower articulation angles, only necessary to accommodate suspension travel. The tripot joint has the advantage of easily accommodating 'plunge', i.e., allowing changes in effective shaft length. The Rzeppa joint is a true CV joint, and is better able to accommodate the large misalignment due to steering motions, and so is better suited to the outboard end of the shaft.

There are other styles of CV joints available as well; notable for its complexity, the Thompson joint (see Watson et al [5]) is composed of coincident universal joints, with pantograph control linkages to ensure equal angles of articulation, and the Clemens scissors mechanism discussed in Masarati and Morandini [6]. A schematic of a scissors joint with four arms is shown in Fig. 3a.

3. MODELLING

This paper discusses the tangent stiffness matrix of a CV joint. In order to describe the mechanics, one must define the *medial plane* of the joint. The medial plane orients itself such that the angle of the misalignment between the two shafts is bisected the plane, as shown in Fig. 3b. The moment that is transmitted through the CV joint must remain normal to the medial plane.

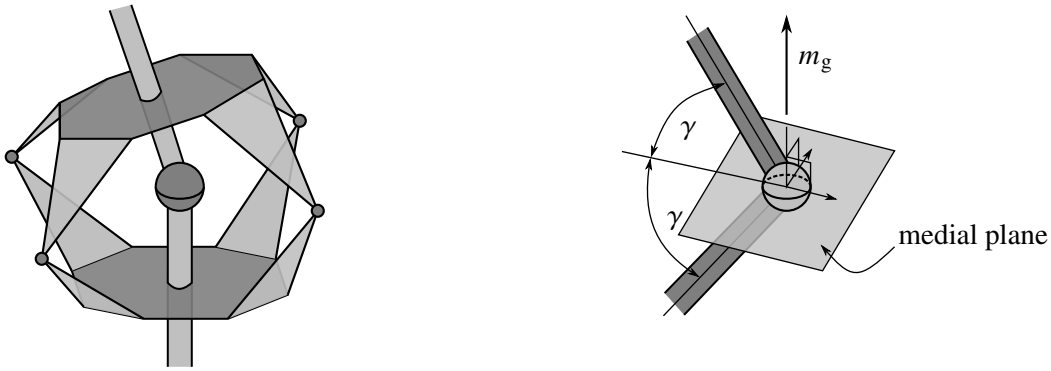

(a) A a Clemens scissors joint with four arms.

(b) Generic CV joint, showing the medial plane.

Fig. 3. Schematic diagrams of CV joints.

The proposed tangent stiffness matrix of the single-point CV joint is shown in Eq. (13). The matrix contains all the same terms as for the spherical joint, plus the terms for the moment. Because the moment changes direction to remain normal to the medial plane between the two shafts, terms depending on the angular motion of both bodies appear. The term of interest is $0.5\tilde{\boldsymbol{m}}_g$. Note that when considering the medial plane of the CV joint, that said plane will rotate by precisely half the angular motion of the body. Thus, the component of the moment that acts in the rotated reference frame will be based on half the difference in the rotation of the two bodies.

$$\mathbf{K} = -\begin{bmatrix} \mathbf{0} & \tilde{\boldsymbol{f}}_g & \mathbf{0} & \mathbf{0} \\ \mathbf{0} & \tilde{\boldsymbol{r}}_1\tilde{\boldsymbol{f}}_g + 0.5\tilde{\boldsymbol{m}}_g & \mathbf{0} & -0.5\tilde{\boldsymbol{m}}_g \\ \mathbf{0} & \mathbf{0} & \mathbf{0} & -\tilde{\boldsymbol{f}}_g \\ \mathbf{0} & 0.5\tilde{\boldsymbol{m}}_g & \mathbf{0} & -\tilde{\boldsymbol{r}}_2\tilde{\boldsymbol{f}}_g - 0.5\tilde{\boldsymbol{m}}_g \end{bmatrix} \tag{13}$$

4. NONLINEAR ANALYSIS

A simple geometric analysis of the Clemens scissor joint can be done to compare the linearized result to the true nonlinear behaviour. Consider two bodies attached by a spherical joint at point A, as shown in Fig. 4. Allow that a moment N and its equal and opposite reaction moment act on the two bodies as shown.

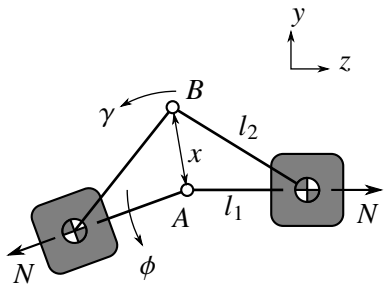

$$\gamma = \phi/2 \tag{14}$$

$$N = fx\cos\gamma \tag{15}$$

$$M = fx\sin\gamma = N\tan(\phi/2) \approx N\phi/2 \tag{16}$$

Fig. 4. A schematic of diagram of two bodies attached by a CV joint; a simple analysis shows that the off-axis moment increases as a tangent function of half the angle of misalignment.

An arm is attached to each of the two bodies with a pin joint; the two arms are attached by a second spherical joint at point B. The lengths l_1 and l_2 are fixed, and the point B is located a varying distance x from point A. If one of the two bodies is displaced by an angle ϕ as shown in the figure, the point B must move to accommodate, but by symmetry, the angle γ locating B must be simply half of ϕ. Allowing that the forces acting along the x axis (out of the page) at both points A and B create moments around both the y and z axes (M and N, respectively), the moment N can by found as a function of ϕ.

If the angle ϕ is taken as small, then the resulting expression can easily be linearized. An examination of the tangent function shows that the second order term in the Taylor expansion is zero, and the next term is third order. As a result, the linear approximation of the moment M is accurate to within 10% at angles as large as $\phi = 60°$. A differentiation then shows that the result is in agreement with Eq. (13).

$$\frac{dM}{d\phi} = 0.5N \tag{17}$$

5. EXAMPLE PROBLEM

A simple example problem is proposed to demonstrate the application of the CV joint. Two rigid bodies with identical properties are aligned along the z axis, and attached together via a CV joint of varying style. The example uses a mass of $m = 1$ kg, all moments of inertia are $I = 1\ \mathrm{kg\,m^2}$, the cross-products of inertia are all zero, and the distance from the mass centre to the CV joint is $r = 1$ m.

Each body is additionally fixed to the ground via a spherical joint. The lower body is fixed at its mass centre, while the upper body is fixed a distance $r = 1$ m above its mass centre. The distance from the CV joint to the ground fixed joint was purposely chosen to be different for each body to ensure that the medial plane of the CV joint does not remain in the x-y plane as the system articulates. The spherical joint of the upper body is allowed to slide on the z axis so system is not over-constrained. Equal and opposite constant ground fixed torques act on the bodies such that the CV joint is loaded. The moment acting is $t = 1$ Nm. Weight forces are ignored.

The CV joint in the example is modelled using seven different approaches. First, it is treated as single-point constraint element using the stiffness matrix defined above. Then, to verify the results for the point joint model, the scissors type CV is modelled as a comparison. The scissors joint is modelled as a composite joint, i.e., constructed using a combination of other simple constraints. In this case, there are two possibilities: 1) a combination of a spherical joint at the centre, with dummy (i.e., massless) rigid bodies representing the 'arms' of the joint, hinged to the shaft, and additional spherical joints to connect the dummy bodies, or 2) a combination of a spherical joint at the centre, with massless links, connecting dummy point masses which replace the outer spherical joints.

It is not a requirement that the scissors joint use four arms as shown in the figure; it will operate identically with any number of arms, assuming the geometry of each arm is identical. In fact, even though in practice the joint would typically use multiple arms for symmetry and strength considerations, this causes redundancy in the constraint, and can pose challenges for some modelling formulations. Because the formulation in EoM can accommodate redundant constraints, the scissors joint was modelled using four different approaches. Both of the approaches described above were implemented, each with one arm and no redundancy, and with two arms, on opposing sides of the joint. Of course, as the number of arms increases, the number of dummy bodies also increases, which in turn increases the dimension of the resulting stiffness matrix.

In the sixth variation, the joint is modelled as a compound mechanism using a spherical joint and two massless links. The links lie in the medial plane when the joint is undeflected. Finally, in the last variation, a typical universal joint is modelled as a compound joint using two coincident hinges and a massless dummy intermediate body.

It is noteworthy that the stiffness matrices produced in each case are shown prior to the elimination of the redundant equations and reduction to minimal coordinates. Despite the varying sizes of the stiffness matrix in the different versions of the model, all variations had only three degrees of freedom. The shafts are free to rotate around the z axis, and to deflect into both the x and y directions.

5.1. Single-point CV joint

The single-point joint is modelled according to stiffness matrix given by Eq. (13). For a two body problem, with the point joint model, a 12×12 stiffness matrix is generated. In order to present some of the larger systems, only the form of matrix is presented, i.e., only non-zero entries are indicated, as shown in Fig. 5. Each small square in the figure represents a 3×3 submatrix, and the dots represent a single non-zero entry. Although it is not apparent from the figure, the result is not symmetric; the off-diagonal entries are equal and opposite.

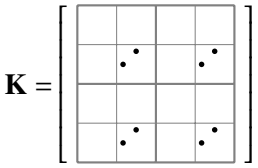

Fig. 5. The stiffness matrix using a point CV joint.

5.2. Scissor, point mass, links, one arm

When implementing the scissors joint with one arm and massless link constraints, there are now three rigid bodies, which gives an 18×18 stiffness matrix. However, the third rigid body is used as the point mass, and so has all rotations constrained, resulting in three rows and columns (16–18) of zeros in the stiffness matrix, as seen in Fig. 6.

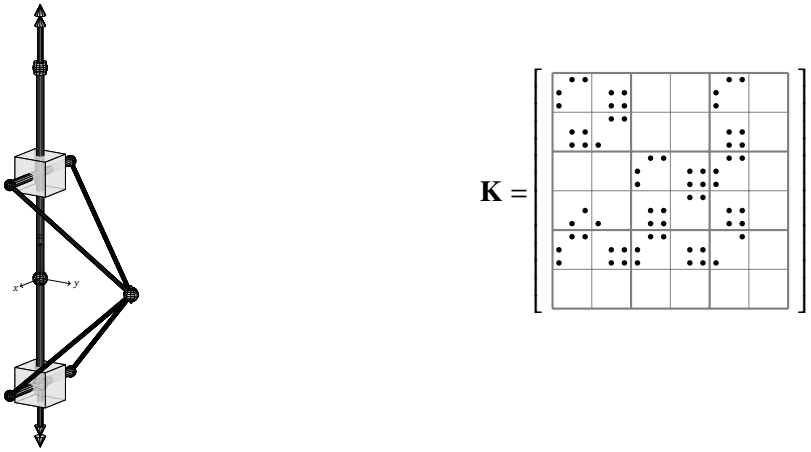

Fig. 6. The stiffness matrix using a single arm scissors joint, modelled using massless links and a dummy point mass.

5.3. Scissor, rigid bodies, hinges, one arm

When implementing the scissors joint with one arm and massless rigid bodies hinged to the shaft, there are now four rigid bodies, which gives a 24×24 stiffness matrix. Interestingly, all of the stiffness terms result in moments rather than forces, so rows 1–3, 7–9, 13–15, and 19–21 are all zeros in the stiffness matrix, as

seen in Fig. 7. Because the arms are modelled as massless rigid bodies, the location of the mass centre is arbitrary, having no effect on the resulting dynamic behaviour. For this model, the centres of mass of both arms were located intermediately between the hinges and the spherical joint. The location of hinge axis of the arms is chosen as offset from the shaft centreline.

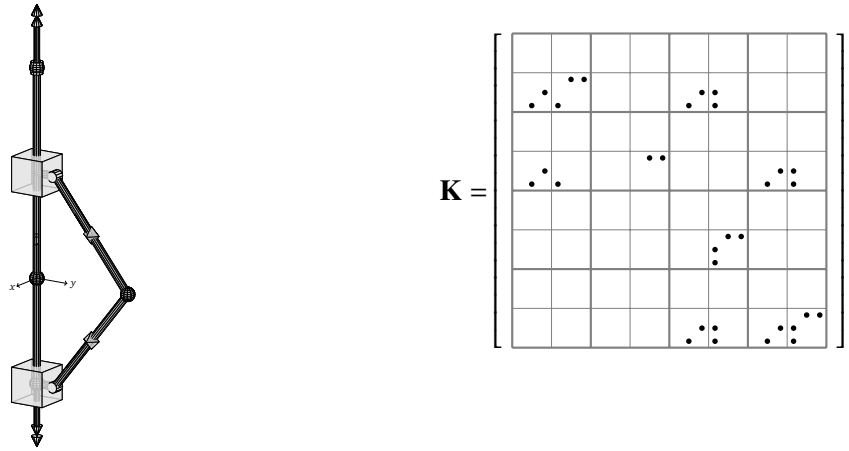

Fig. 7. The stiffness matrix using a single arm scissors joint, modelled using dummy rigid bodies, hinges, and spherical joints.

5.4. Scissor, point mass, links, two arms

When implementing the scissors joint with two arms and massless link constraints, there are also four rigid bodies, which again gives an 24×24 stiffness matrix. However, the third and fourth rigid bodies are used as point masses, and again have all rotations constrained, resulting in six rows and columns (16–18, 22–24) of zeros in the stiffness matrix, as seen in Fig. 8.

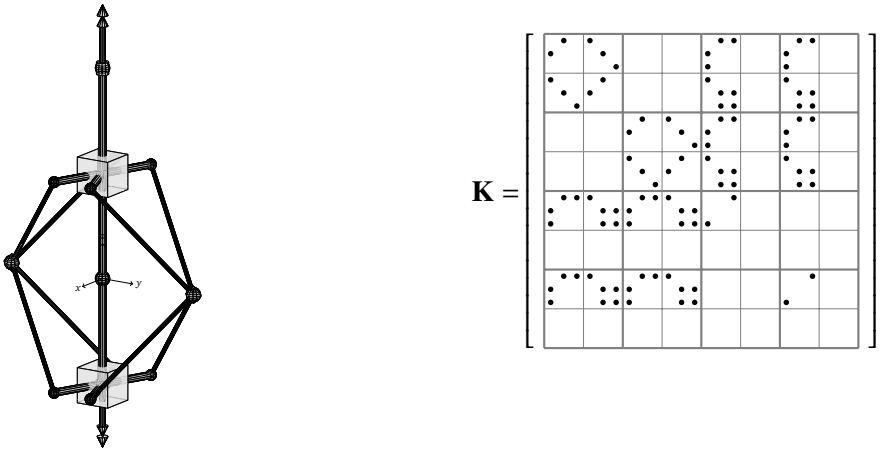

Fig. 8. The scissors joint with two arms, modelled using massless links and a dummy point mass, and the resulting stiffness matrix.

5.5. Scissor, rigid bodies, hinges, two arms

The dual arm scissors joint using rigid bodies gives six rigid bodies, and a 36×36 stiffness matrix. Again, only moments are generated by the stiffness matrix, giving zeros in rows 1–3, 7–9, 13–15, 19-21, 25–27,

and 31–33, as seen in Fig. 9.

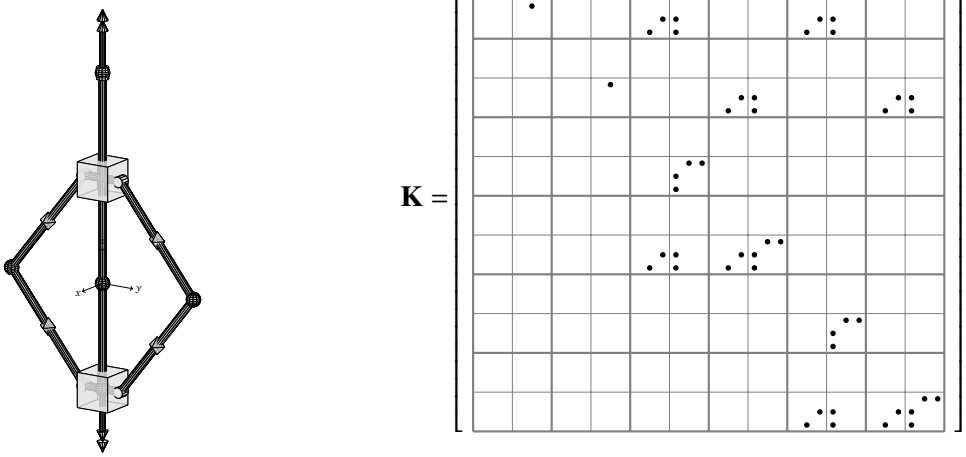

Fig. 9. The dual arm scissors joint, modelled using dummy rigid bodies, hinges, and spherical joints, and the resulting stiffness matrix.

5.6. Planar linkage

As a third comparison, a connection based only on a single central ball joint and two massless links is included as well. The two massless links initially lie in a common plane defined by the central spherical joint and the ends of the links. The behaviour of the joint is interesting, as a single arm connection does not behave equivalently, and two or more links are required, even though the joint contains redundant constraints. Additionally, the ends of the links must be located such that they are co-linear with the central ball joint and the ends other link, e.g., one one body, the link ends lie on the x and y axes, and on the other body on the -x and -y axes. In effect, the arms on each shaft are oriented 90° apart. Because the massless links arms are modelled as constraints and not bodies, the stiffness matrix reduces in size again to 12×12, as seen in Fig. 10. The matrix again is not symmetric, as some of the off axis entries are equal and opposite.

5.7. Universal joint

Finally, a system using a standard universal joint is modelled. The system uses one massless rigid body, and two coincident hinges that are arranged with their axes mutually orthogonal. The model has three rigid bodies and an 18×18 stiffness matrix, given in Fig. 11. The result is notably sparse.

6. LINEAR ANALYSIS

All the variations of the model, with the exception of the universal joint, were found to be equivalent, despite the varying form of the equations. The solution of the resulting equations of motion gave identical eigenvalues of $s = 0$, (twice), and $s = \pm 0.3536 \pm 0.3536\mathrm{i}\ \mathrm{s}^{-1}$, corresponding to a natural frequency $\omega_\mathrm{n} = 0.0796$ Hz, a damping ratio of $\zeta = \pm 0.7071$, a time constant of $\tau = \pm 2.8284$ s, and wavelength of $\lambda = 17.77$ s.

The two zero eigenvalues correspond to a rigid body mode, where both bodies rotate only around the z axis. The remaining eigenvalues indicate that the motion has an unstable oscillatory mode. While perhaps initially surprising, this can be explained if one considers the reaction moment of the CV joint. As soon

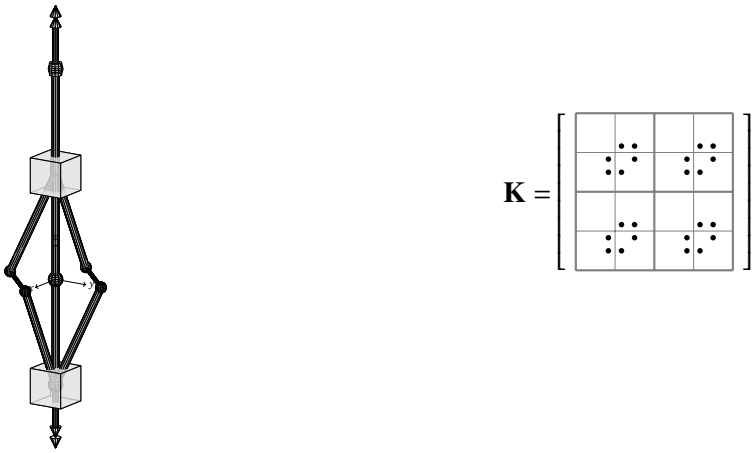

Fig. 10. A connection that uses a single ball joint and two massless links. The links are arranged in a specific manner such that the endpoints are co-linear with the central ball joint and the ends of the opposing link.

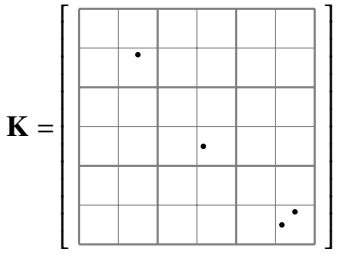

Fig. 11. The stiffness matrix using a universal joint.

as the body experiences any rotation, the applied moment and the reaction moment in the CV become misaligned, and therefore no longer equal and opposite. This results in a small component of the reaction moment acting about a horizontal axis, oriented in a direction perpendicular to the axis disturbance rotation. This unbalanced moment causes a rotation about the perpendicular axis, which in turn generates a moment around the original axis of the disturbance. An examination of the eigenvector of the unstable mode uncovers a 'whirling' type motion, where the joint orbits around the z axis in a rapidly increasing radius spiral.

The eigenvalues of the system using the universal joint are different; two eigenvalues are again zero, two are purely imaginary, and two are equal and opposite real, indicating an exponential instability. The imaginary eigenvalue pair is $s = 0 \pm 0.8409\text{i}\ \text{s}^{-1}$, and the real pair are $s = \pm 0.8409\ \text{s}^{-1}$. The imaginary pair correspond to a natural frequency of $\omega_\text{n} = 0.1338$ Hz and a wavelength of $\lambda = 7.472$ s, while the real pair represent a time constant of $\tau = \pm 1.1892$ s. The free solution of the equations of motion displays only planar motion; the whirling seen in the other systems is not present.

7. CONCLUSIONS

From the results generated, several conclusions can be drawn. First, it is apparent the proposed point CV joint formulation is equivalent to the other compound joints, while also providing a much more compact model. Next, it is clear that the use of redundant constraints in the scissors joint with multiple arms does not negatively affect the behaviour of the model, although the increase in size of the model is certainly a disadvantage. Also, it is clear that the two planar link model provides another mathematically compact alternative to the scissors joint, while again providing equivalent behaviour. While not fully described above,

experiments suggest that this planar model requires multiple arms, and therefore redundant constraints, in order to provide equivalent behaviour. Furthermore, the geometry of the links must be chosen carefully to maintain this behaviour. Cases in which the geometry was varied to break the co-linear condition described above resulted in differing behaviour. Finally, it is clear that even for cases where the misalignment is small, the dynamic behaviour of the universal joint is not equivalent to the behaviour of a CV joint.

REFERENCES

1. Minaker, B. and Rieveley, R. "Automatic generation of the non-holonomic equations of motion for vehicle stability analysis." *Vehicle system dynamics*, Vol. 48, No. 9, pp. 1043–1063, 2010.
2. Minaker, B. "The tangent stiffness matrix in rigid multibody vehicle dynamics." *Mathematical and Computer Modelling of Dynamical Systems*, Vol. 21, No. 3, pp. 288–310, 2015.
3. Rzeppa, A.H. "Universal joint." US Patent 1,916,442, July 4 1933.
4. Urbinati, F. and Pennestrì, E. "Kinematic and dynamic analyses of the tripode joint." *Multibody System Dynamics*, Vol. 2, No. 4, pp. 355–367, 1998.
5. Watson, I., Gangadhara Prusty, B., Olsen, J. and Farrell, D. "A parameter investigation into the thompson constant-velocity coupling." *Journal of Mechanical Design*, Vol. 133, No. 12, 2011.
6. Masarati, P. and Morandini, M. "An ideal homokinetic joint formulation for general-purpose multibody real-time simulation." *Multibody System Dynamics*, Vol. 20, No. 3, p. 251, 2008.